HIGH THROUGHPUT MULTIPLEX IMAGE ANALYSES FOR ANDROGEN RECEPTOR FUNCTION

Adam T. Szafran, Marco Marcelli, Michael A. Mancini*

Department of Molecular and Cellular Biology, and the Michael DeBakey VA Hospital*
Baylor College of Medicine, Houston, TX

ABSTRACT

Evidence suggest that a subgroup of patients affected by either prostate cancer or androgen insensitivity syndrome harbor mutations within the androgen receptor that may contribute to the disease phenotype. To characterize the effects of these AR mutations, we have developed a high content screening assay able to determine AR transcriptional activity, cellular distribution, and cellular patterning simultaneously at the single cell level. We demonstrate that two mutations (F764L, R840C) isolated from AIS patients retain the ability to achieve similar levels of transcriptional activity, nuclear translocation, and nuclear hyperspeckling as wild type receptor, but require significantly higher levels of agonist. Differences in responses seen between the different compounds tested also suggest that the assay could be amendable to agonist screening for personalized patient drug selection.

Index Terms— high content screen, androgen receptor, androgen insensitivity syndrome

1. INTRODUCTION

The combination of automated fluorescence microscopy and automated image analyses, commonly referred to as high content screening (HCS), has been an emerging technology in the pharmaceutical industry and, more recently, in academic settings. The ability to capture and analyze thousands of image fields per day has removed many of the traditional sample limitations associated with manual microscopy. Furthermore, with vast amounts of image data available for "data mining, increasingly complex quantitative analyses have led to number of more complex HCS assays. Collectively, these efforts have been a key harbinger for high throughput systems biology [1].

The androgen receptor (AR), a prototypical member of the nuclear receptor (NR) superfamily that binds testosterone, is important in the development and maintenance of the male sexual phenotype under normal physiological conditions. Alterations in this signaling pathway are associated with diseases such as androgen insensitivity syndromes (AIS) and prostate cancer, the 2nd leading cause of cancer related deaths in males [2, 3]. It has been suggested that with both diseases, there exist a subpopulation of patients that harbor mutations within AR that might be associated with the increased receptor signaling observed in prostate cancer, or the decreased androgen responsiveness in AIS patients [4-6]. While effects of these mutations can be determined in various population-based biochemical assays (e.g., DNA binding, protein interactions, transcriptional reporter gene activity), these approaches fail to account for the heterogeneous nature of the cellular populations and results from disparate experiments are difficult to assemble into a systems-level understanding of mechanism(s).

To this end, we have developed an image-based HCS assay to examine mutation-specific effects upon AR signaling in the presence of various compounds. Using a four-channel fluorescence approach we report here quantitative results for multiple aspects of AR intracellular biology at the single cell level. We have recapitulated wild-type (WT) AR and several AR mutations in HeLa cells using green fluorescent protein (GFP) fusions (GFP-WTAR, GFP-AR F764L, GFP-AR R840C). To measure AR transcriptional activity adapted the mammalian probasin promoter-derived construct ARR2PB to drive expression of a red fluorescent protein reporter (dsRED2skl). This multiplex approach allows us to simultaneously quantify changes in AR nuclear translocation, nuclear patterning, and transcriptional activity in response to compounds. Automated fluid-handling, image acquisition and analyses of GFP-AR HeLa in a 96 well plate format demonstrate differential AR responsiveness to several androgens, including restoration of normal cellular trafficking and transcription function of AIS AR F764L and AR R840C using supraphysiological doses of ligands.

2. RESULTS

Assay System

To study the various AR mutations in an equivalent environment, we selected the HeLa cell line to transiently transfect with the various GFP tagged receptors. HeLa cells are easy to transfect, lack endogenous AR and most other nuclear receptors that could yield off-target responses, and

have growth properties that make them ideal for imaging work. Furthermore, microarray RNA expression analysis demonstrated that GFP-AR expressed in HeLa cells is able to regulate (induce or repress) known AR regulated genes suggesting that HeLa cellular machinery supports AR transcriptional regulation. In order to visualize AR transcriptional regulation, we used a pARR-2PB-dsREDskl reporter construct which is based on the AR-responsive composite probasin promoter [7]. Induction of AR transcriptional regulation results in the nuclear translocation of the GFP-tagged receptor and expression of a dsRED2skl protein targeted to the cell's peroxisomes (Figure 1).

To screen for mutation specific effects on compound responses, HeLa cells were transiently transfected with both the GFP-AR expression vectors and the reporter construct and then plated onto optical bottom 96 well assay plates (Cytowell, Nunc). After allowing the cells to adhere to the plates, cells were incubated for 18hr with a 11-point titration of the compound of interest. After incubation was complete, plates were fixed, nuclei stained using DAPI, and cell stained using CellMask (Invitrogen). The compound titration, compound addition to the cell plates, plate fixation, and staining were performed using a Beckman Biomek NX liquid handling robotic platform. Cells were imaged using an automated microscope (Beckman IC-100) with a 40X/0.90 NA objective. For each field, four images were captured: a DAPI image (nuclei), a green image (GFP), a red image (dsRED2skl reporter), and a far red image (CellMask, cell borders). In order to obtain a high Z' score using only cells expressing physiological levels of AR, 64 40x fields were collected from each well.

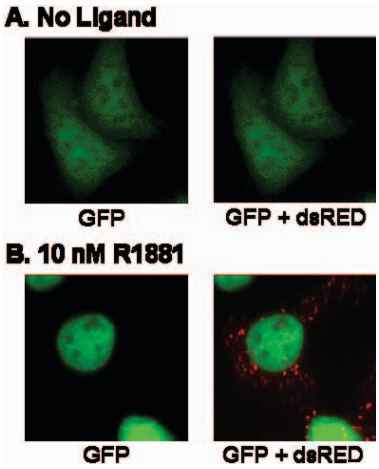

Figure 1. HeLa cells transfected with GFP-WT AR and the pARR-2PB-dsREDskl reporter construct. Cells were imaged after either no treatment (A) or 10nM R1881 for 18 hr (B)

Image Analysis

To analyze the images, we used Pipeline Pilot software (Accelrys) with advanced image analysis components to identify individual cells. Nuclear masks were generated by applying a series of thresholding, distance transformation, and watershed operations to the DAPI image (Figure 2A). Cell masks were generated by applying a similar series of thresholding, smoothing, and watershed operations to the CellMask image (Figure 2B). The cell mask processing operations make use of the nuclear masks to define individual objects and assume one nucleus per cell. Once both nuclear and cell masks are determined, a third region consisting of only the cytoplasm is calculated (Figure 2C). All regions are then overlaid on background-subtracted GFP and dsRED2skl images to extract quantitative data

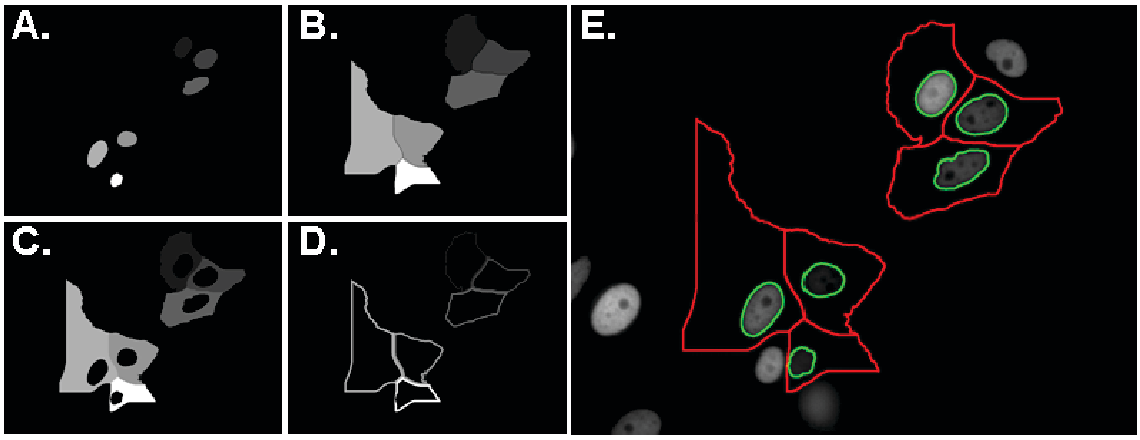

Figure 2. Automated analysis of images collected by automated microscopy. The Pipeline Pilot protocol generates masks for each individual nuclei (A), cell (B), cytoplasm (C), and cell edge (D). The generated masks are overlaid on background subtracted GFP-AR (E) and dsRED2skl images to quantify changes in AR cellular distribution and reporter accumulation. Objects potentially on edge of image are removed from image analysis. Cells that were expressing AR at levels 2-fold higher than in LnCAP cells were exclued from the analysis; typically, only 80% of the GFP-AR positive cells were used.

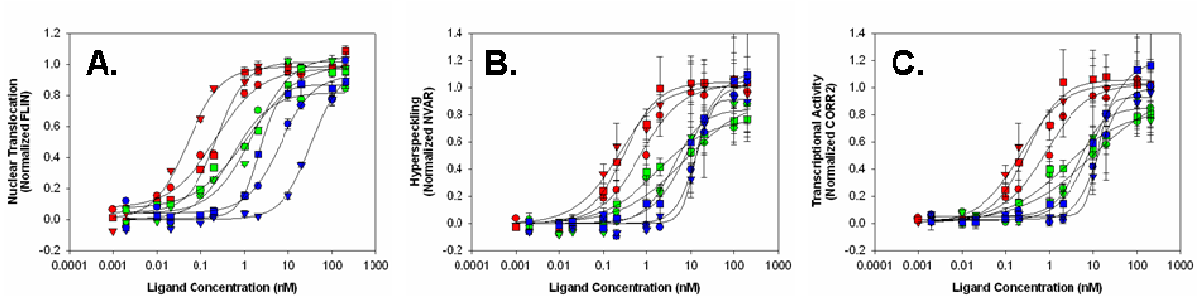

Figure 3. AR with either the AR F764L or the AR R840C mutation demonstrate reduced sensitivity to AR agonists, but are able to achieve similar maximal responses as wild type receptor at high ligand concentrations. Plots show observed AR nuclear translocation (A), nuclear hyperspeckling (B), or transcriptional activity (C) of wild type AR(**red**), AR F764L (**blue**), or AR R840C (**green**) in response to DHT (○), R1881(▽), or mibolerone (□).

describing AR cellular distribution within the cytoplasm and nucleus, and the accumulation of the transcriptional reporter protein (Figure 2E). Mitotic, apoptotic, and cell clusters are eliminated from analysis by applying filters based on nuclear area, nuclear circularity, and nuclear area to cell area ratio. Importantly, we also selected for a subpopulation of HeLa cells expressing AR at levels comparable to that found in LNCaP cells using techniques described elsewhere [8].

Because the transfected HeLa cells have a wide range of GFP-AR expression which result in image artifacts in neighboring cells expressing little or no AR (e.g., spill-over of fluorescence), we also calculate a fourth region for each cell which consist of a thin (10 pixel wide) band around the perimeter of the calculated cell region (Figure 2D). By comparing the average GFP intensity in this region to that found within the cytoplasm of the cells, we determine an Edge_Ratio for each cell. Cells free from neighboring fluorescence spill-over artifact will have a low Edge_Ratio whereas cells adjacent to highly overexpressing cells will have a high Edge_Ratio; cells from this latter group are eliminated from analysis.

To analyze the GFP-AR subcellular trafficking and transcription results, three key features were determined for each cell: 1) degree of nuclear translocation (**f**raction of GFP signal **l**ocalized **i**n **n**ucleus(FLIN)); 2) amount of

Table 1: EC50 (nM) Values of Observed Responses

Compound	Structure	Response*	WTAR	AR F764L	AR R840C
DHT	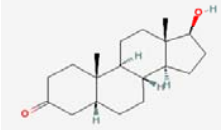	NT	0.22 ± 0.03	6.5 ± 2.0	0.52 ± 0.12
		HYP	0.74 ± 0.15	12.26 ± 1.03	6.93 ± 1.6
		TA	0.82 ± 0.16	13.6 ± 1.2	10.1 ± 1.7
R1881	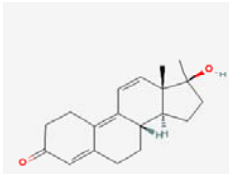	NT	0.05 ± 0.01	3.7 ± 1.2	1.52 ± 0.46
		HYP	0.28 ± 0.06	13.4 ± 1.5	3.97 ± 0.93
		TA	0.30 ± 0.05	12.2 ± 0.5	4.67 ± 1.0
Mibolerone	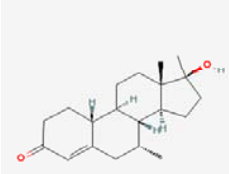	NT	0.23 ± 0.04	2.14 ± 0.18	1.23 ± 0.32
		HYP	0.30 ± 0.05	9.55 ± 1.06	1.76 ± 0.61
		TA	0.31 ± 0.06	11.0 ± 0.7	2.27 ± 0.88

* NT - Nuclear Translocation, HYP - Hyperspeckling, TA - Transcriptional activity

nuclear hyperspeckling (**n**uclear **var**iation of GFP signal intensity (NVAR)); and, 3) transcriptional activity (total amount of **corr**elated channel **2**/dsRED2skl signal (CORR2)). The ability to measure the hyperspeckled patterning is important because it may represent the formation of transient protein complexes by the receptor as it scans the DNA for androgen response elements [9, 10].

Assay Quality and Repeatability

To ensure that the automated image analysis protocols maintain acceptable performance for the entire image set, the developed protocol is tested against a sample image set comprised of randomly-selected fields from control wells (5%), and experimental wells (1%). Acceptable performance is defined as >90% accurate object identification as determined by visual inspection. Overall assay quality and repeatability was determined using methods described elsewhere [11]. Z' values were 0.49-0.91.

Differential ligand responses of AR F764L and AR R840C

We examined the responses of WT AR, AR F764L, and AR R840C to the natural androgen, dihydroxytestosterone (DHT), and two synthetic androgens, R1881 and mibolerone. AR F764L carries a mutation within the ligand binding domain (LBD) of AR and was identified in a patient with complete androgen insensitivity (CAIS, [12, 13]). AR R840C carries a R838C/R840C mutation also within the LBD and was identified in a patient with partial androgen insensitivity (PAIS; [12, 13]). With WT AR, all compounds induced significant nuclear translocation, nuclear hyperspeckling, and transcriptional reporter protein accumulation (Figure 3, Table 1). EC50 values for the responses ranged between 0.05 ± 0.01 nM and 0.82 ± 0.16 nM. For AR F764L, all three compounds were able to induce near-equivalent maximal responses similar to WT AR, but only at higher concentrations (range = 0.52 – 10.1 nM, Figure 3, Table 1). For example, the EC50 for nuclear translocation with R1881 was 0.05 nM with WT AR and 1.52 nM with AR F764L. For AR R840C, maximal responses were decreased 15-21% compared to WT AR, and these values were attained at concentrations intermediate between those for WT AR and AR F764L (range = 2.14 – 13.6 nM, Figure 3, Table 1). These results correlate well with the severity of the observed phenotype and demonstrate that both AR F764L and AR R840C can be induced to demonstrate near-normal AR function, but only with supra-physiological levels of agonist.

3. CONCLUSIONS

We describe here a new HCS assay to rapidly characterize multiple aspects of AR function, and how mutations and compounds can have differential effects. The results presented here describe how both the AR F764L and AR R840C mutants may attain near-wildtype AR functionality, but only at supraphysiological levels of agonist. Differential responses to different agonists also suggest that the assay could be amendable to agonist screening for personalized patient drug selection. We are currently in the process of adapting our assay system to screen for the same responses in genital skin fibroblasts isolated directly from AIS patients. Finally, combined with current RNAi technologies, this multiplex single cell assay should also aid in the identification of proteins involved in pathways that regulate AR biology (Szafran, Marcelli and Mancini, in preparation).

4. REFERENCES

[1] Lee, S. & Howell, B.J. High-content screening: emerging hardware and software technologies. *Methods Enzymol* **414**, 468-483 (2006).

[2] Quigley, C.A. et al. Androgen receptor defects: historical, clinical, and molecular perspectives. *Endocr Rev* **16**, 271-321 (1995).

[3] Jemal, A. et al. Cancer statistics, 2006. *CA Cancer J Clin* **56**, 106-130 (2006).

[4] Poletti, A., Negri-Cesi, P. & Martini, L. Reflections on the diseases linked to mutations of the androgen receptor. *Endocrine* **28**, 243-262 (2005)

[5] Mohler, J.L. et al. The androgen axis in recurrent prostate cancer. *Clin Cancer Res* **10**, 440-448 (2004).

[6] Marcelli, M., Lamb, D.J., Weigel, N.L. & Cunningham, G.R. in Androgens in health and disease. (eds. C. Bagatell & W.J. Bremner) 157-189 (Humana Press, Totowa; 2003).

[7] Zhang, J.F., Thomas, T.Z., Kasper, S. & Matusik, R.J. A small composite probasin promoter confers high levels of prostate-specific gene expression through regulation by androgens and glucocorticoids *in vitro* and i*n vivo*. *Endocrinology* **141**, 4698-4710 (2000).

[8] Marcelli, M. et al. Quantifying effects of ligands on androgen receptor nuclear translocation, intranuclear dynamics, and solubility. *J Cell Biochem* **98**, 770-788 (2006).

[9] Metivier, R., Reid, G. & Gannon, F. Transcription in four dimensions: nuclear receptor-directed initiation of gene expression. *EMBO Rep* **7**, 161-167 (2006).

[10] van Royen, M.E. et al. Compartmentalization of androgen receptor protein-protein interactions in living cells. *J Cell Biol* **177**, 63-72 (2007).

[11] Morelock, M.M. et al. Statistics of assay validation in high throughput cell imaging of nuclear factor kappaB nuclear translocation. *Assay Drug Dev Technol* **3**, 483-499 (2005).

[12] Quigley, C.A., et al. Androgen receptor defects: historical, clinical, and molecular perspectives. *Endocr Rev* **16**, 271-321 (1995)

[13] Marcelli, M., Zoppi, S., Wilson, C.M., Griffin, J.E. & McPhaul, M.J. Amino acid substitutions in the hormone binding domain of the human androgen receptor alter the stability of the hormone-receptor complex. *J Clin Invest* **94,** 1642-1650 (1994)